Contract No:

This document was prepared in conjunction with work accomplished under Contract No. DE-AC09-08SR22470 with the U.S. Department of Energy (DOE) Office of Environmental Management (EM).

Disclaimer:

SRNL®
SAVANNAH RIVER NATIONAL LABORATORY
OPERATED BY SAVANNAH RIVER NUCLEAR SOLUTIONS

December 26, 2019 SRNL-STI-2019-00636, Rev. 1

TO: B. T. BUTCHER, 773-42A

FROM: T. L. DANIELSON, 773-42A

REVIEWER: J. A. DYER, 773-42A

A LIMITED-IN-SCOPE COMPARISON OF SUBSIDENCE SCENARIOS FOR 3D VADOSE ZONE PORFLOW TRENCH MODELS[1]

Summary

This technical memorandum summarizes the results from two separate sequences of 3D PORFLOW vadose zone flow and contaminant transport models that were used to test the impact of different spatial distributions of subsidence boundary conditions. More specifically, the two simulation setups used a general conceptual model for an engineered trench (ET): one with a subsided region specified in the center of the trench and one with a subsided region located at the end of the trench. Both subsided regions had the same geometric specifications (e.g., length, width, orientation), but used water infiltration rate boundary conditions that appropriately accounted for surface runoff and lateral drainage from the adjacent upslope intact regions of the final closure cap. Because of the substantially higher water infiltration rate associated with the subsided region at the end of the trench, this geometry produced higher absolute peak fluxes to the water table for all six radionuclides that were simulated. However, the slower release rate of the centrally located subsided hole geometry produced a higher flux to the water table in the time period subsequent to the absolute peak. A third model was implemented as a control, where the water infiltration rate that corresponds to the centrally located subsided region was applied at the end of the trench to highlight the purely geometric effects. The results show that a higher water infiltration rate produces a sharper peak, while a lower infiltration rate leads to a broader peak. A centrally located hole impacts more of the waste zone, producing a higher peak when an equal infiltration rate is applied. These generalized qualitative differences, and their impacts on the overall modeling workflow (i.e., from vadose zone models to limits and dose calculations), should receive appropriate consideration during the development of conceptual models.

[1] In this revision, a typographical error was corrected in equation 2 so that the first term reads "I_B", rather than "I_I".

Discussion

Background

In a previous investigation, Dyer (2018) identified a bounding conceptual infiltration model for the E-Area Low-Level Waste Facility (ELLWF) final closure cap. The bounding model represents a central section of the final closure cap as shown in Figure 1 that captures the minimum (150 feet) and maximum (585 feet) slope lengths for the entire cap. Water infiltration estimates for this final closure cap geometry were provided for both intact and subsided conditions, where the subsided infiltration rate is a function of the surface runoff and lateral drainage from the upslope intact area of the cap.

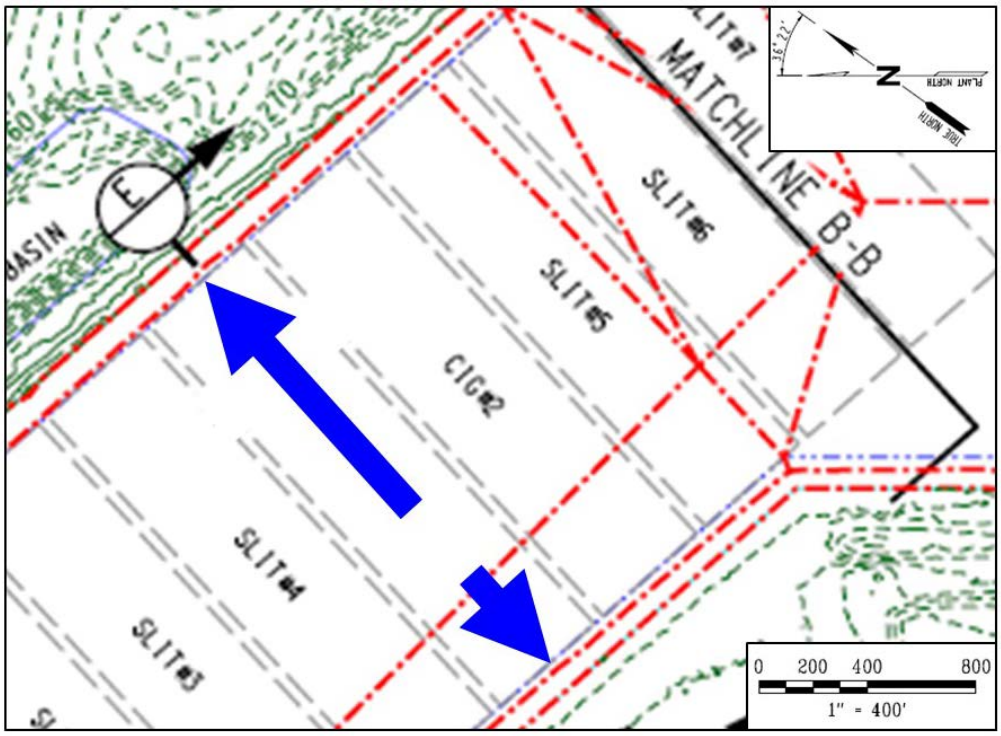

Figure 1. The portion of the ELLWF final closure cap represented by the bounding conceptual infiltration model. Red dashed lines highlight the spatial extent and relevant features of the final closure cap design and long and short blue arrows show the flow direction of runoff for the long and short slopes.

In the development of the conceptual model framework for Slit and Engineered Trenches (ST/ETs) to be used in the next revision of the ELLWF Performance Assessment (PA), one unresolved model feature is the spatial distribution of subsidence boundary conditions. In general, the greatest likelihood of cap subsidence for ST/ETs is expected to occur at locations where non-crushable packages have been placed;

however, these locations are not precisely known and vary on a trench-by-trench basis. Due to the sloped nature of the final closure cap, the spatial location of a subsided hole is relevant because the corresponding subsided water infiltration rate increases as a function of the upslope intact area. For this reason, any subsided region located at the end of a disposal unit footprint will have the highest possible water infiltration rate within the bounding infiltration model geometry.

In a recent study (Danielson, 2019), a stochastic approach was employed using historical crushable/non-crushable inventory data, as well as the geometric constraints associated with ST/ETs, to provide insights into the most likely spatial distribution(s) of subsidence in current and future ST/ETs. The results of that investigation revealed that non-crushable packages are likely to appear along the edges, and in some cases, localized central regions of the trench. Notably, this was a purely geometric study that did not account for the actual timing of package placements, but rather relied on statistical package distributions for a predefined percent subsidence scenario. Subsequent communications with Solid Waste Management led to them providing the actual package placement dates for all non-crushable packages (see data in Appendix A). Using the operational start and end dates for each trench segment (an ET is considered a single segment) as a temporal frame of reference, the fractional package placement time was computed as:

$$f = \frac{t_{Package} - t_{TrenchOpen}}{t_{TrenchOpen} - t_{TrenchClose}} \quad (1)$$

where, $t_{Package}$, $t_{TrenchOpen}$, and $t_{TrenchClose}$ are the times (expressed as a real number) that the package was placed, the trench was opened for operations, and the trench segment was closed, respectively. Based on Equation 1, it was assumed that any package with an f-value less than or equal to 0.05 or greater than or equal to 0.95 (i.e., the package was placed within the first 5% or 95% of the operational timeline) had a high probability of being located at one end of the trench segment. Some of the trench segments are centrally located in the overall disposal unit footprint and, therefore, these data were further distilled down to consist of only those packages that have a high probability of falling at the end of the segments that lie along the end of the disposal unit footprint. Of the 154 non-crushable packages listed, approximately 13% are speculated to reside at end locations based solely on the timing of placement. The current work seeks to provide insights on the potential impacts of a model geometry with a subsided area (or hole) located at the end of the disposal unit footprint (i.e., the location with the highest possible water infiltration rate) in order to better understand the relevance of including such a geometry in the next revision of the ELLWF PA. A model geometry with a hole located at the center of the disposal unit footprint (i.e., with a more moderate water infiltration rate) will be used for comparison.

Model Inputs and Assumptions

A single model geometry and mesh were used to simulate both the central and end subsided locations, thereby reducing the possibility of differences in the peak flux to the water table that might result from numerically solving the flow and/or transport equations. The 3D model geometry is shown in Figure 2 and Figure 3 in the XY- and XZ-planes, respectively. Material properties were defined using SRNL's most up-to-date hydraulic property data package (Nichols, 2019). The interim and final covers overhang the edge of the disposal unit footprint by 10 feet and 40 feet, respectively, in the x-direction, while both covers extend across the model domain in the y-direction. The interim cover is applied for an institutional control period of 100 years assuming a constant infiltration rate boundary condition. The final cover is installed at the end of institutional control and assumes an intact infiltration rate everywhere except for either one of the two labeled subsided regions (shown in green and numbered in Figure 2).

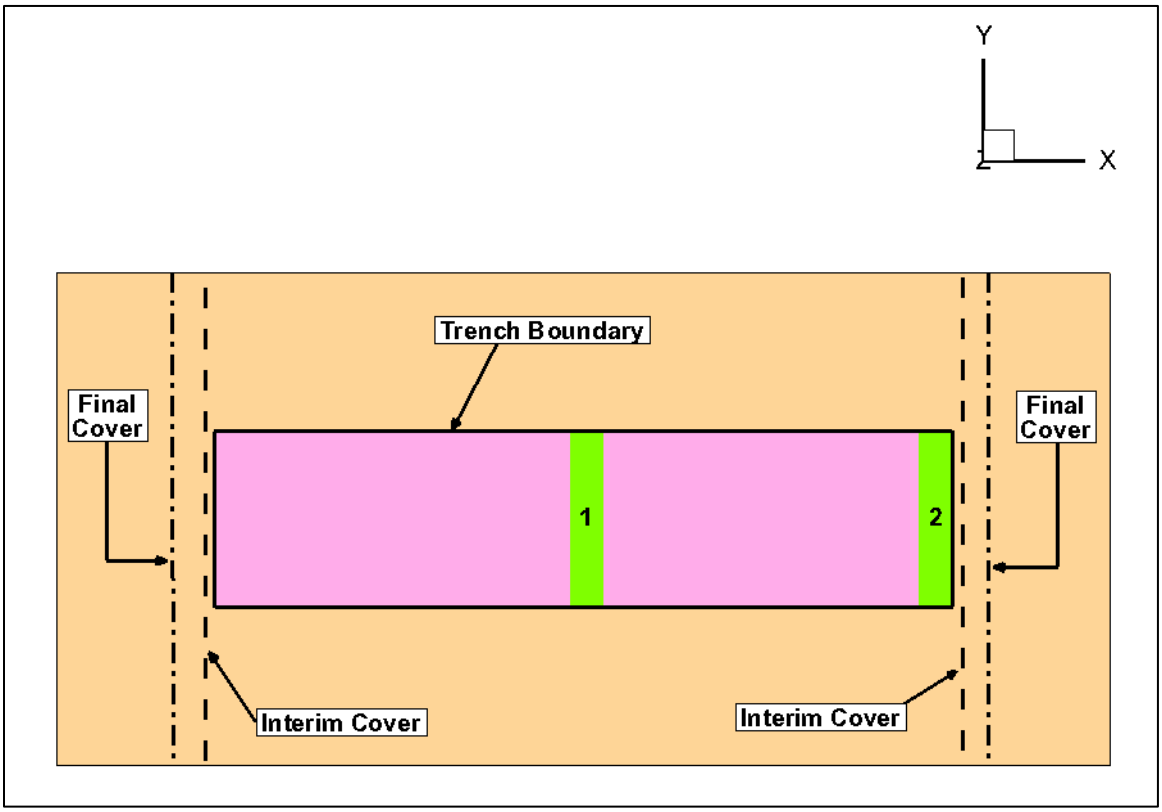

Figure 2. Schematic of the model geometry with the boundaries of the final cover, interim cover, and (green and numbered) subsided regions at the center and end of the disposal unit shown.

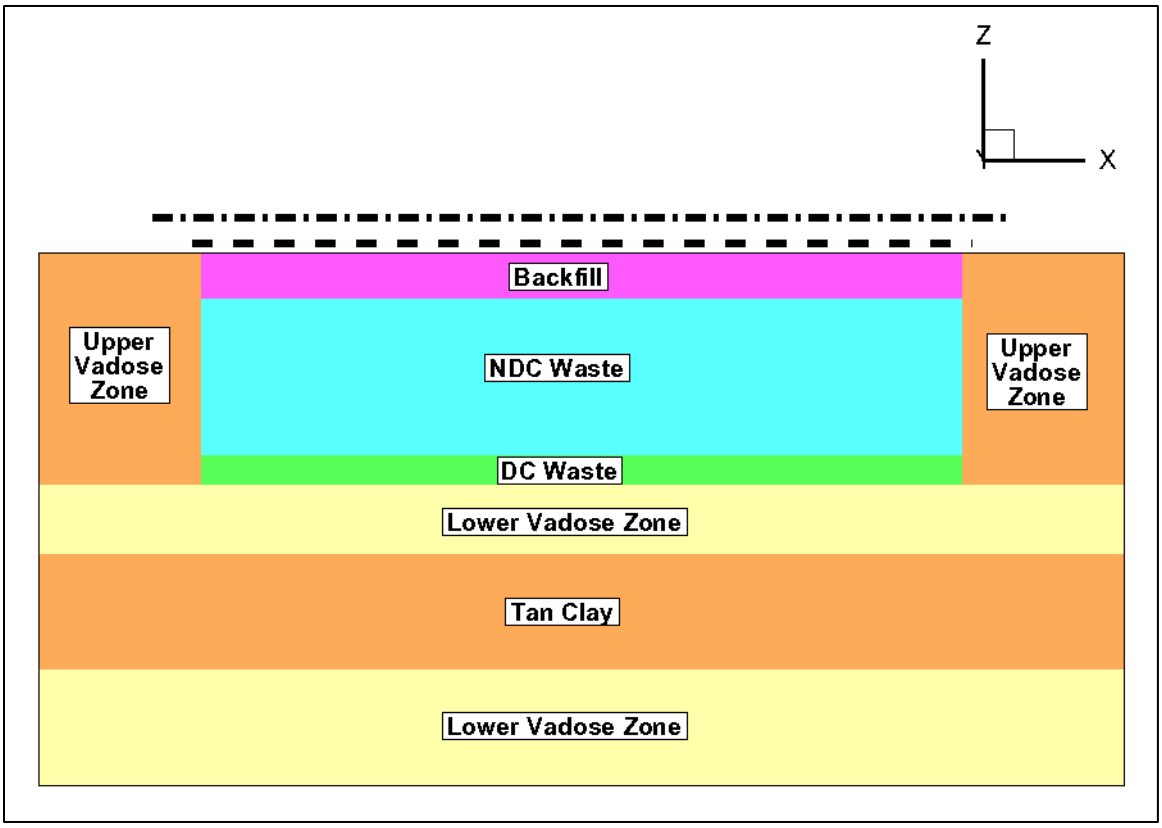

Figure 3. Schematic of the model geometry with material zones from the ground surface to the water table labeled and the spatial extent of the interim and final covers indicated by the dashed and dashed-dotted lines, respectively.

Table 1 displays the time-dependent intact infiltration rate as reported by Dyer and Flach (2018); subsided-area infiltration rates were back calculated for each hole location based on the upslope intact-to-subsided area ratio using the relationship:

$$I_S = I_B + \frac{L_U}{L_H}(I_B - I_I) \tag{2}$$

where I_I is the intact infiltration rate, L_U is the length of the intact upslope area, L_H is the length of the subsided region (both lengths are measured in the direction parallel to surface runoff), and I_B is the closure-cap-specific subsidence scenario background infiltration rate (i.e., annual-average rainfall minus annual-average evapotranspiration), which is 16.5 inches per year in the current work.

Table 1. Intact and subsided infiltration rates for subsided regions at the end and central locations. Background infiltration rate refers to all portions of the model that are not covered by the final closure cap.

Relative Year	Background Infiltration Rate (inches/year)	Intact Infiltration Rate (inches/year)	Subsided Infiltration Rate End (inches/year)	Subsided Infiltration Rate Center (inches/year)
Operation	15.78	15.78		
0-100	15.78	0.1		
100	15.78	0.00088	449.60	164.99
180	15.78	0.0079	449.42	164.93
290	15.78	0.19	444.67	163.30
300	15.78	0.20	444.27	163.16
340	15.78	0.32	441.18	162.10
380	15.78	0.41	438.99	161.35
480	15.78	1.46	411.37	151.88
660	15.78	3.23	364.84	135.93
1100	15.78	7.01	265.48	101.87
1900	15.78	10.65	170.07	69.15
2723	15.78	11.47	148.48	61.75
3300	15.78	11.53	146.91	61.21
5700	15.78	11.63	144.30	60.32
10100	15.78	11.67	143.20	59.94

To highlight the purely geometric aspects of the subsided hole's location, the infiltration rate that was calculated based on the upslope intact-area-to-subsided-area ratio of the central hole location was applied to the end subsided hole location (in a separate model). Using the infiltration rates from Table 1, a series of 74 unique flow fields, covering a time period of 1271 years, were computed using PORFLOW (ACRi, 2010). Subsequently, flow fields were supplied as inputs to transient contaminant transport simulations where 1 Ci of the source radionuclide was distributed uniformly throughout the disposal unit for Sr-90, H-3, Tc-99, U-235, I-129, and C-14. Initially, all source material was placed in the NDC Waste material zone (see Figure 3), but upon dynamic compaction at the end of institutional control, the waste was transferred to the DC Waste material zone (see Figure 3). Transport simulations were run for 1271 years with one-year time steps to obtain the peak flux to the water table profile for each radionuclide.

In the next revision of the ELLWF PA, radionuclide flux to the water table profiles will be used as source inputs to radionuclide transport simulations in the saturated zone, where the time-dependent concentrations at various points of assessment (e.g., a 100-meter perimeter surrounding the ELLWF) will be used to calculate limits for (to be determined) time windows of interest. Because the flux to the water table is linearly related to the concentration at the points of assessment, the flux to the water table profiles are a strong indicator of how any subsidence scenario will impact the final results (i.e., limits and dose) in the PA. For each subsided hole location in the current analysis, the cumulative radionuclide flux to the water table should be approximately equal across the entire simulation time (exactly equal if enough simulation time passes such that all source material is released from both subsidence geometries). However, because two different infiltration rates are used for the two geometries, the timing of radionuclide transport to the water table may differ. Therefore, when comparing the scenarios, two key details will be investigated: (1) a comparison of the peak concentration for each radionuclide and each subsided hole location and (2) the overall cumulative behavior in a given time window.

Results

In the current section, each of the subsidence scenarios will be discussed using the names corresponding to the descriptions in Table 2.

Table 2. Description of subsidence cases.

Subsidence Scenario Name	***Description***
End	20-foot-long by 157-foot-wide subsided region at the center of the trench footprint (green rectangle labeled "1" in Figure 2) with the subsided infiltration rate for the center as specified in Table 1.
Center	20-foot-long by 157-foot-wide subsided region at the end of the trench footprint (green rectangle labeled "2" in Figure 2) in with the subsided infiltration rate for the end as specified in Table 1.
End with Center Infiltration	20-foot-long by 157-foot-wide subsided region at the end of the trench footprint (green rectangle labeled "2" in Figure 2) with the subsided infiltration rate for the center as specified in Table 1.

Comparisons of the flux to the water table profiles for each subsidence scenario are shown for H-3, I-129, Sr-90, Tc-99, U-235, and C-14 in Figure 4 through Figure 9. Qualitatively, the flux to the water table profiles are quite similar between the three subsidence scenarios: the absolute peaks occur at approximately the same time with the "Center" and "End with Center Infiltration" scenarios both occurring slightly later in time than "End." With the exception of H-3, "End" produces the highest absolute peak for each radionuclide in this investigation. This result is expected because the water infiltration rate is substantially higher and, therefore, higher radionuclide species concentrations are flushed out at each time step when compared to the more gradual release produced by the "Center" scenario.

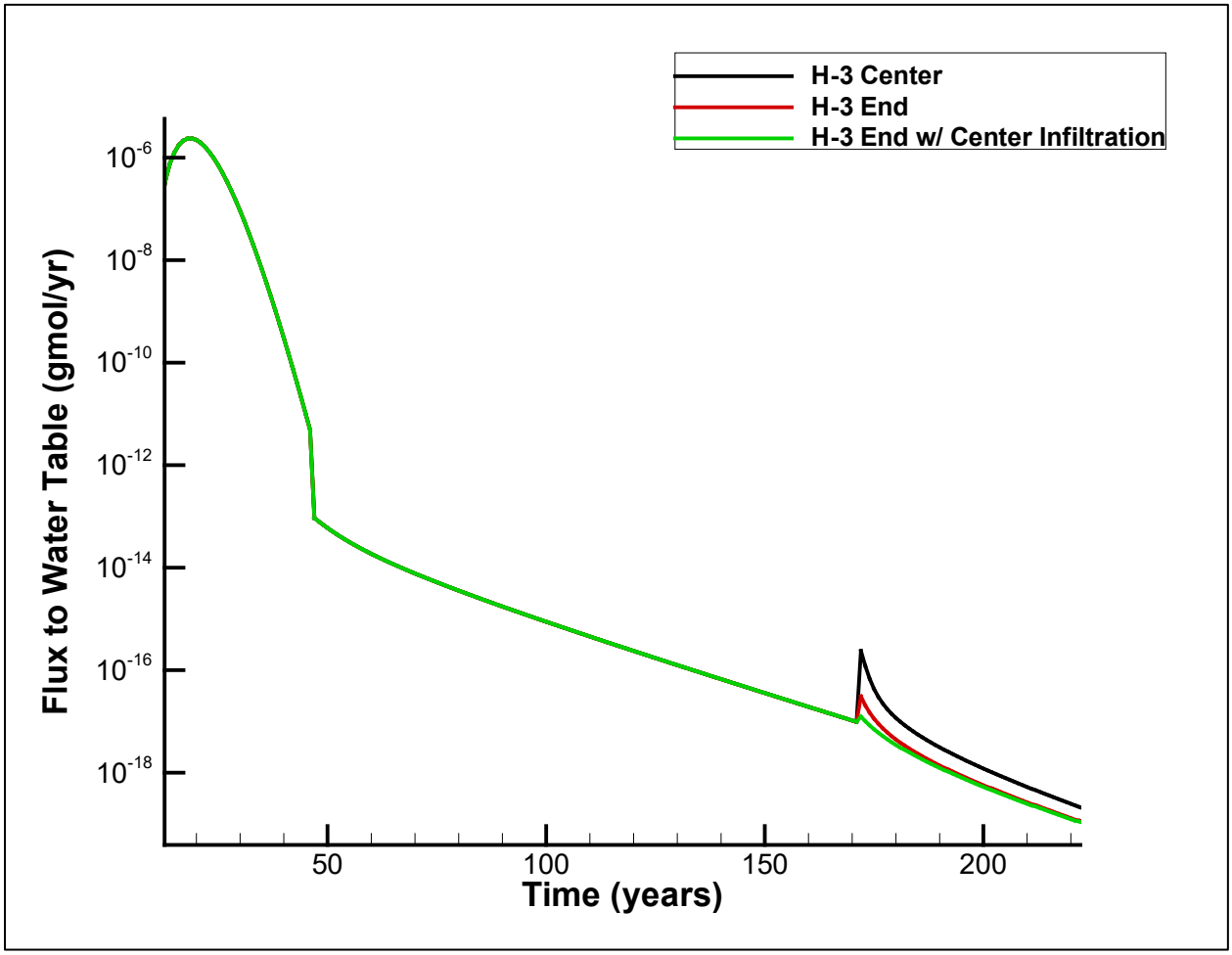

Figure 4. Flux to the water table comparison for a subsided region located in the center of the trench (black), at the end of the trench with the infiltration rate for the end (red), and at the end of the trench with the infiltration rate for the center (green) for H-3.

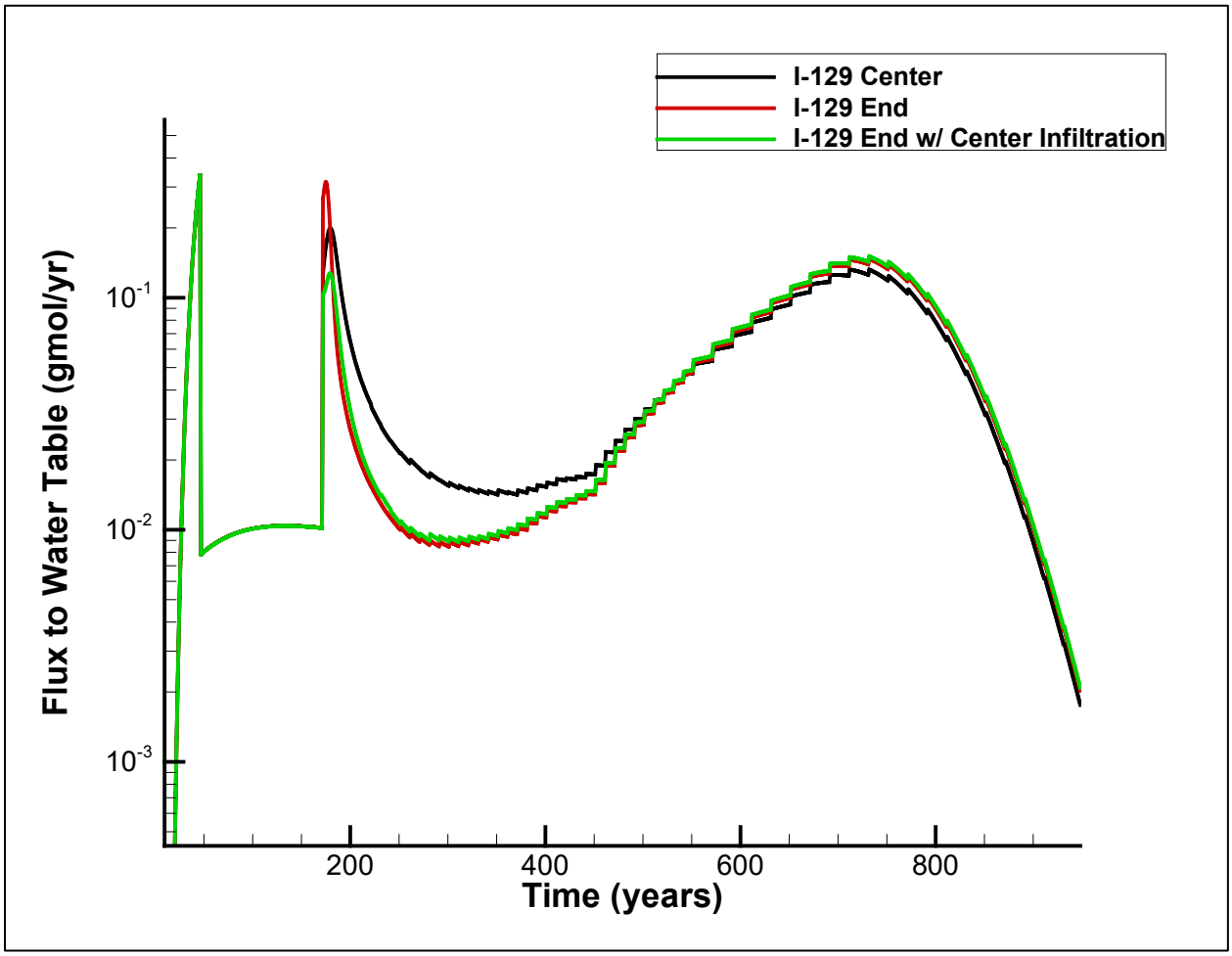

Figure 5. Flux to the water table comparison for a subsided region located in the center of the trench (black), at the end of the trench with the infiltration rate for the end (red), and at the end of the trench with the infiltration rate for the center (green) for I-129.

The "End with Center Infiltration" scenario yields the lowest absolute peaks for all radionuclides, highlighting an important geometric aspect. That is, "Center" allows water to impact a larger volume of waste because the extent of lateral spreading occurs only in regions impacting the waste zone, whereas in the "End" geometry, some of the water spreads outside the disposal unit footprint, thereby impacting no waste at all. This effect is shown in the saturation profiles for the "Center" and "End" scenarios in Figure 10 through Figure 13, where the lateral spread of water through the subsided region impacts approximately half as much waste in the "End" versus the "Center" scenario.

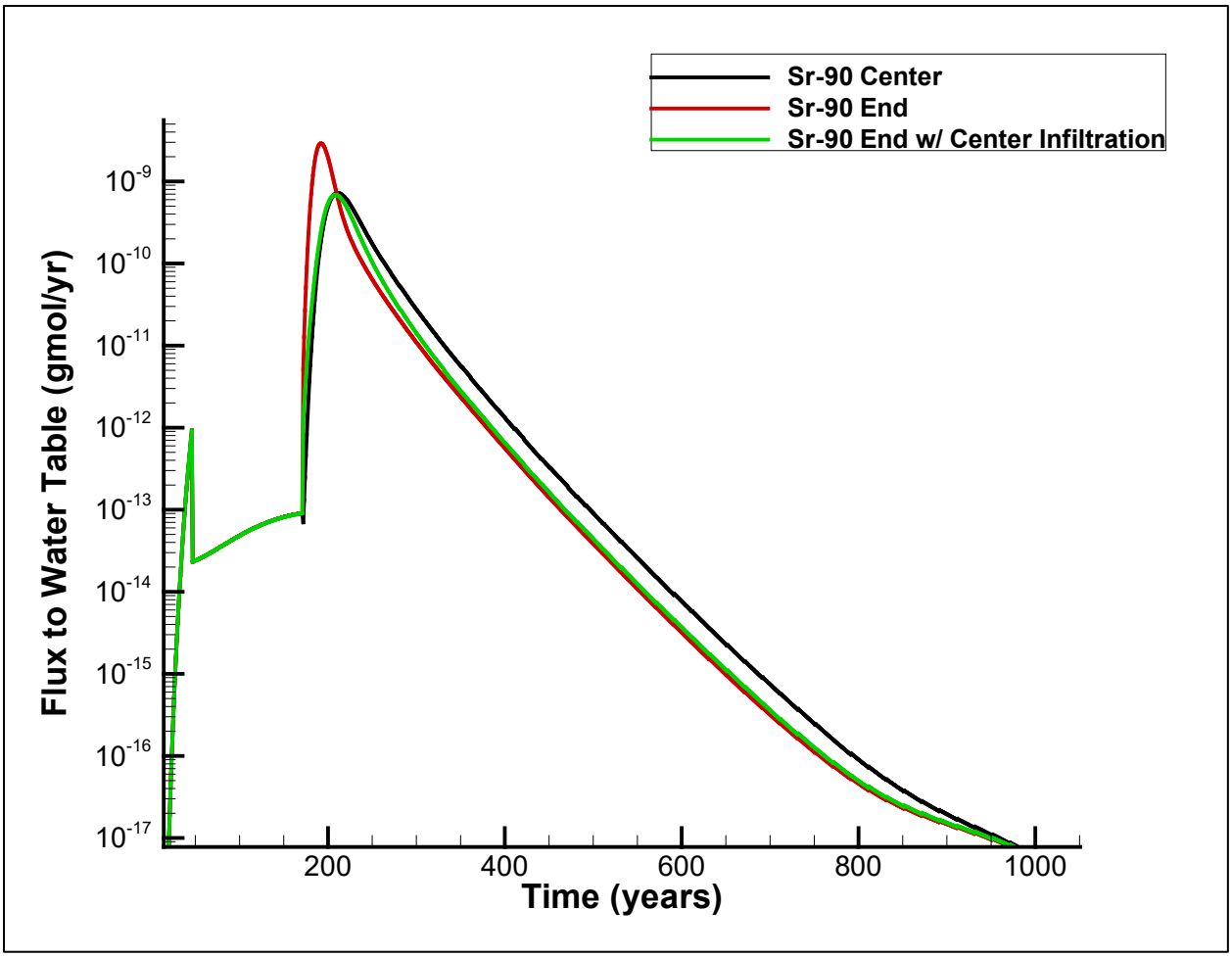

Figure 6. Flux to the water table comparison for a subsided region located in the center of the trench (black), at the end of the trench with the infiltration rate for the end (red), and at the end of the trench with the infiltration rate for the center (green) for Sr-90.

Notably, when there is a secondary peak (e.g., I-129, Tc-99, C-14), the fluxes for both end subsidence cases tend to be higher than for the "Center" scenario, while the "End with Center Infiltration" scenario tends to yield the highest secondary peak. The "Center" scenario produces a more gradual release of radionuclides through time. In contrast, the "End" scenario produces a sharp initial release followed by a significant drop due to a lower available local concentration. The "End with Center Infiltration" scenario releases much less mass initially than the other two scenarios *and* impacts less of the waste zone, therefore retaining more overall radionuclide mass until later in time when the rest of the cap begins to degrade and, consequently, results in a higher secondary peak.

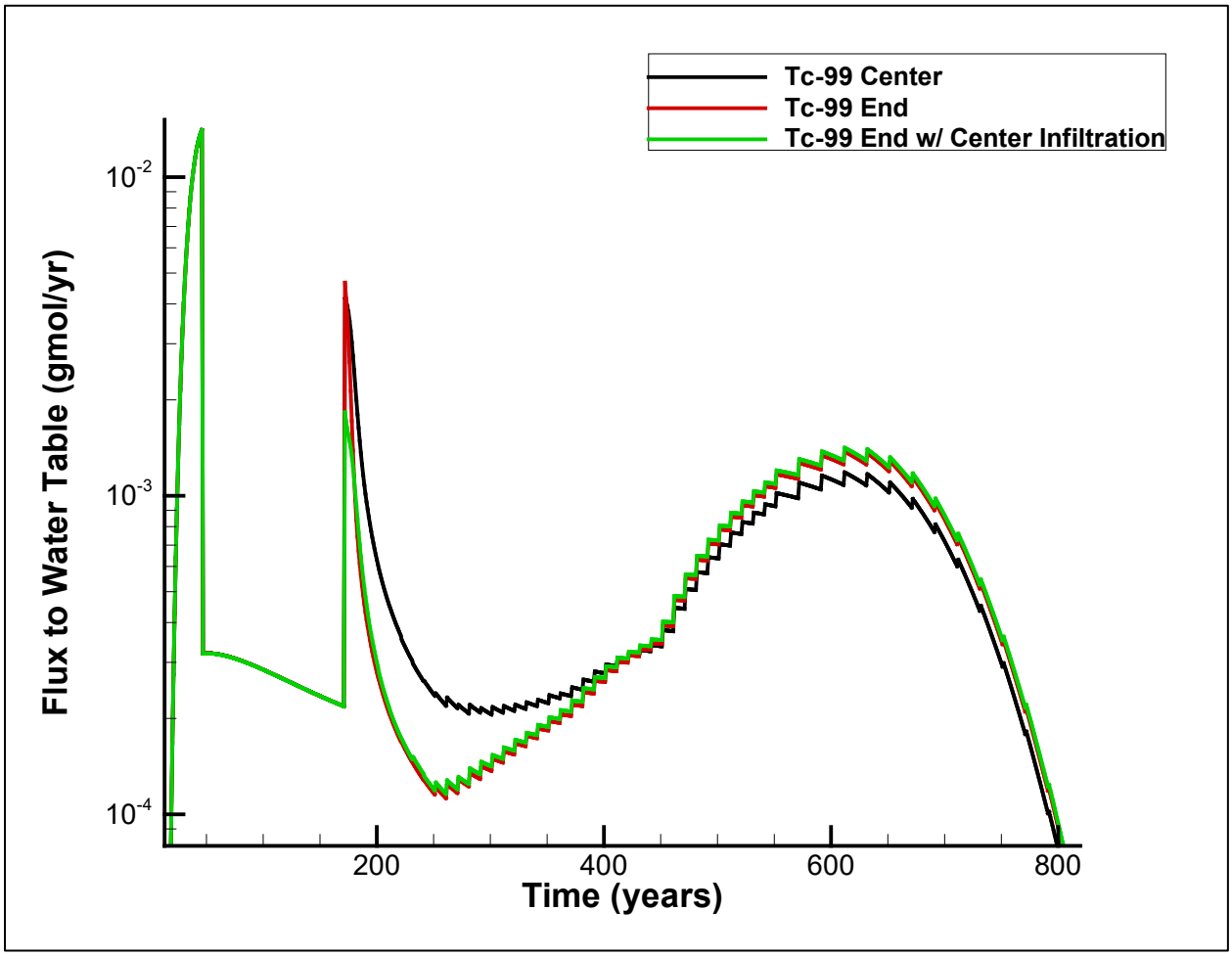

Figure 7. Flux to the water table comparison for a subsided region located in the center of the trench (black), at the end of the trench with the infiltration rate for the end (red), and at the end of the trench with the infiltration rate for the center (green) for Tc-99.

H-3 shows a slightly different behavior than the rest of the radionuclides, where the peak flux to the water table occurs prior to the installation of the final closure cap. Once subsidence occurs, the central subsided hole location leads to the maximum local peak flux. This behavior can also be explained by Figure 10 through Figure 13 where a greater mass of water interacts with unretarded H-3 due to lateral spreading before the waste decays to negligible concentrations. However, this local peak is nearly ten orders of magnitude lower than the absolute peak and, therefore, is considered negligible.

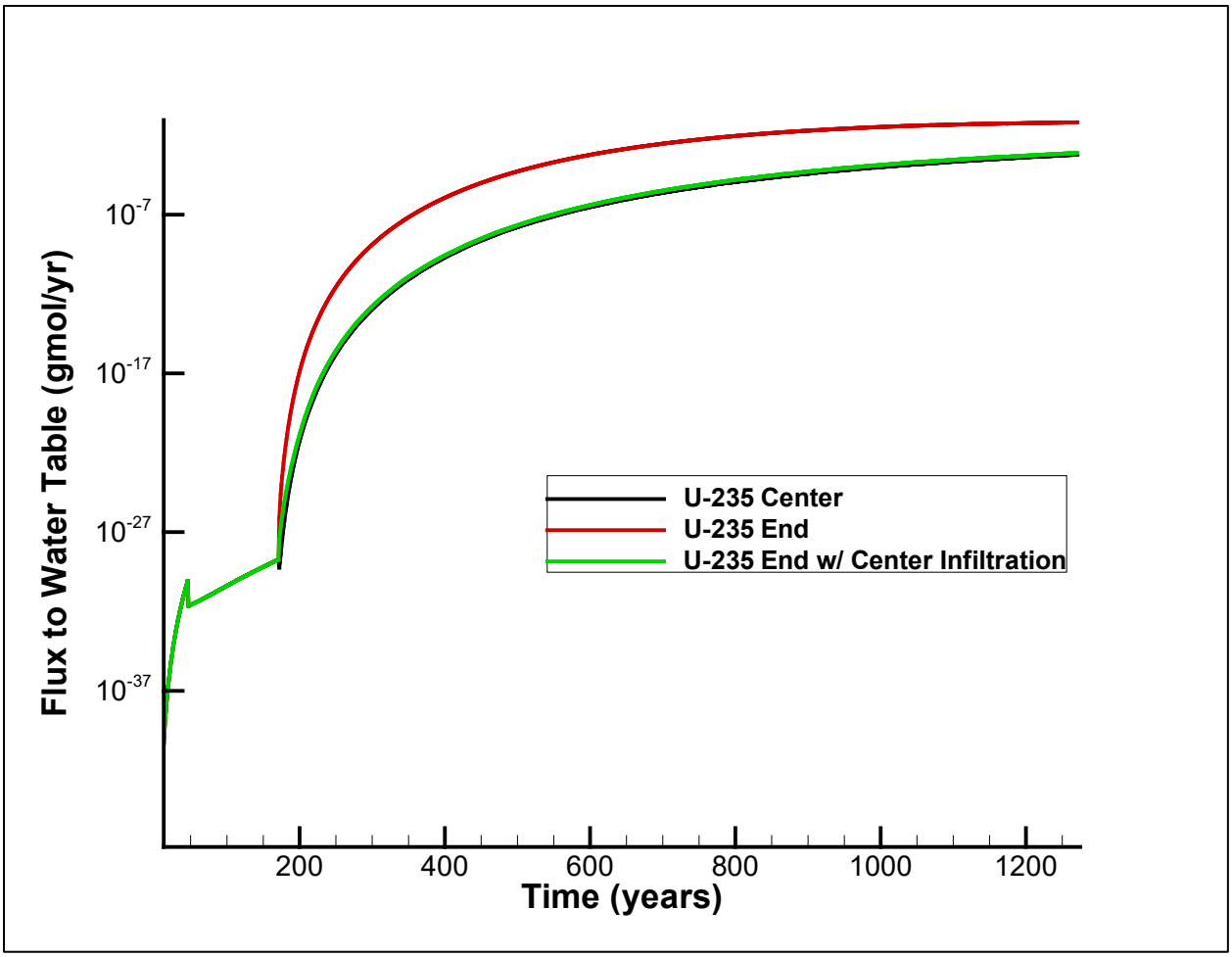

Figure 8. Flux to the water table comparison for a subsided region located in the center of the trench (black), at the end of the trench with the infiltration rate for the end (red), and at the end of the trench with the infiltration rate for the center (green) for U-235.

Profiles of the ratio of flux to the water table at time, *t*, were computed as the flux to the water table for the "End" scenario divided by the flux to the water table for the "Center" scenario and are shown in Figure 14 through Figure 19. These figures are insightful when considering time windows. For any given time, *t*, a ratio of 1.0 indicates that the two fluxes are equal, a ratio greater than 1.0 indicates that the "End" scenario yields a higher flux, and a value less than 1.0 indicates that the "Center" scenario yields the higher flux. While the "End" scenario is shown to produce the highest absolute peak flux to the water table for the current suite of radionuclides, a consequence of this behavior is that in the subsequent time period (which tends to last much longer than the length of time over which the absolute peak occurs), the "Center" scenario produces a higher flux. Using Sr-90 as an example (Figure 16), the absolute peak flux occurs

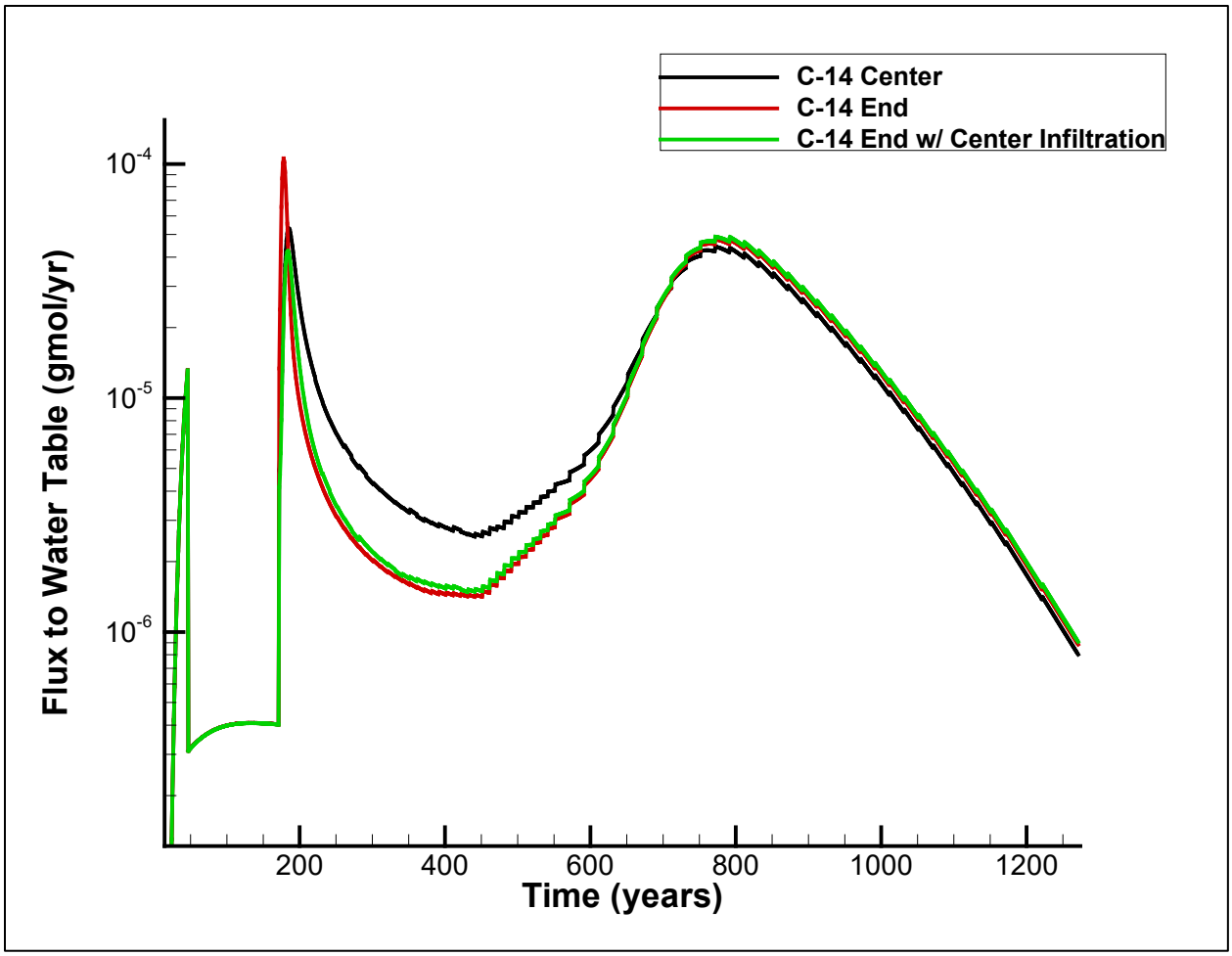

Figure 9. Flux to the water table comparison for a subsided region located in the center of the trench (black), at the end of the trench with the infiltration rate for the end (red), and at the end of the trench with the infiltration rate for the center (green) for C-14.

within a time period of approximately 40 years. During that time period, the ratio indicates that the "End" flux reaches a factor of approximately 100 times greater than the "Center" flux (the absolute peak is a factor of only 4 times greater for "End" compared to "Center"). However, in the subsequent ~600 years, the flux for the "End" scenario remains steady at about one-half of the flux produced by the "Center" scenario. A similar result is shown for each of the radionuclides, where a higher infiltration rate yields a sharper peak and a lower infiltration rate effectively broadens the overall flux to the water table profile.

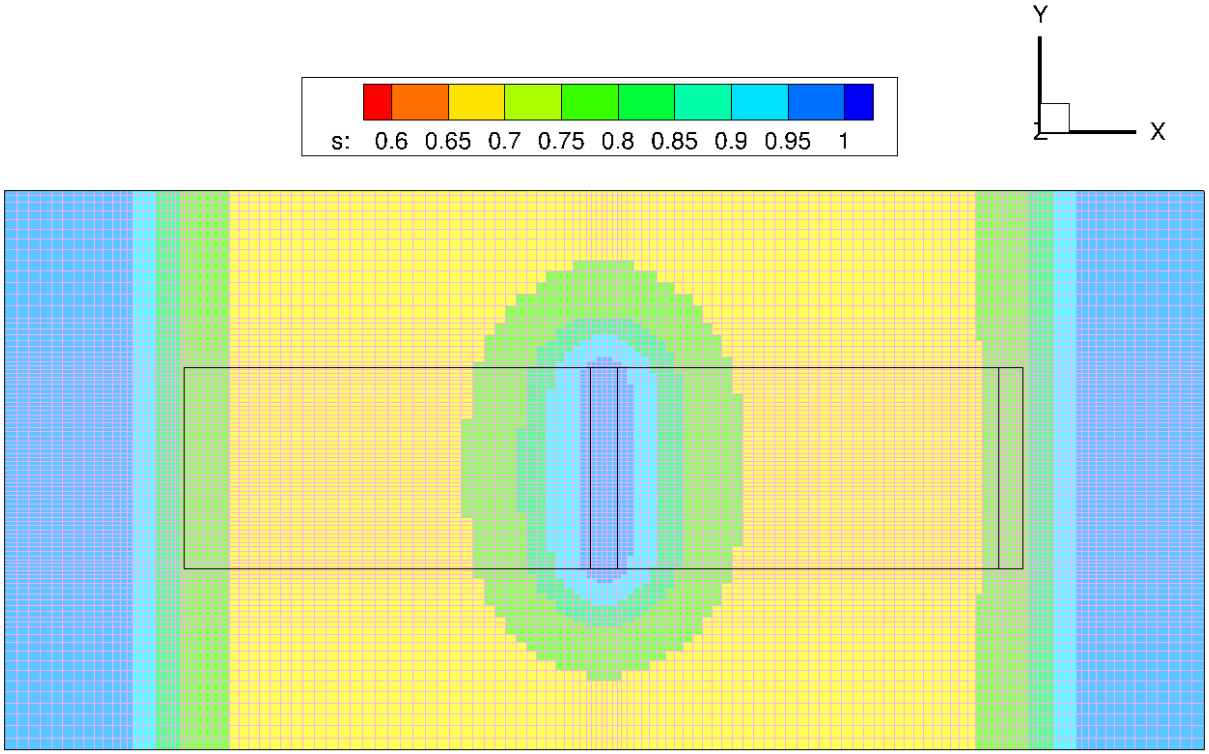

Figure 10. "Center" saturation profile in the surface XY plane (i.e., a "birds-eye-view" of the disposal unit) with the disposal unit footprint and subsidence regions outlined in black.

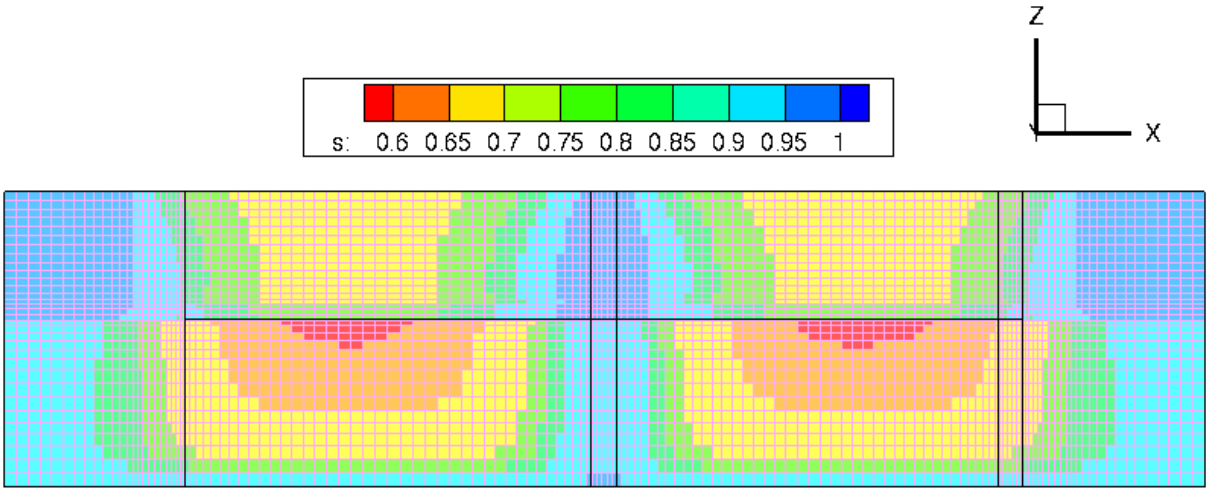

Figure 11. "Center" saturation profile in the middle XZ plane (i.e., a cross-section extending from the ground surface to the water table) with the disposal unit footprint and subsidence regions outlined in black.

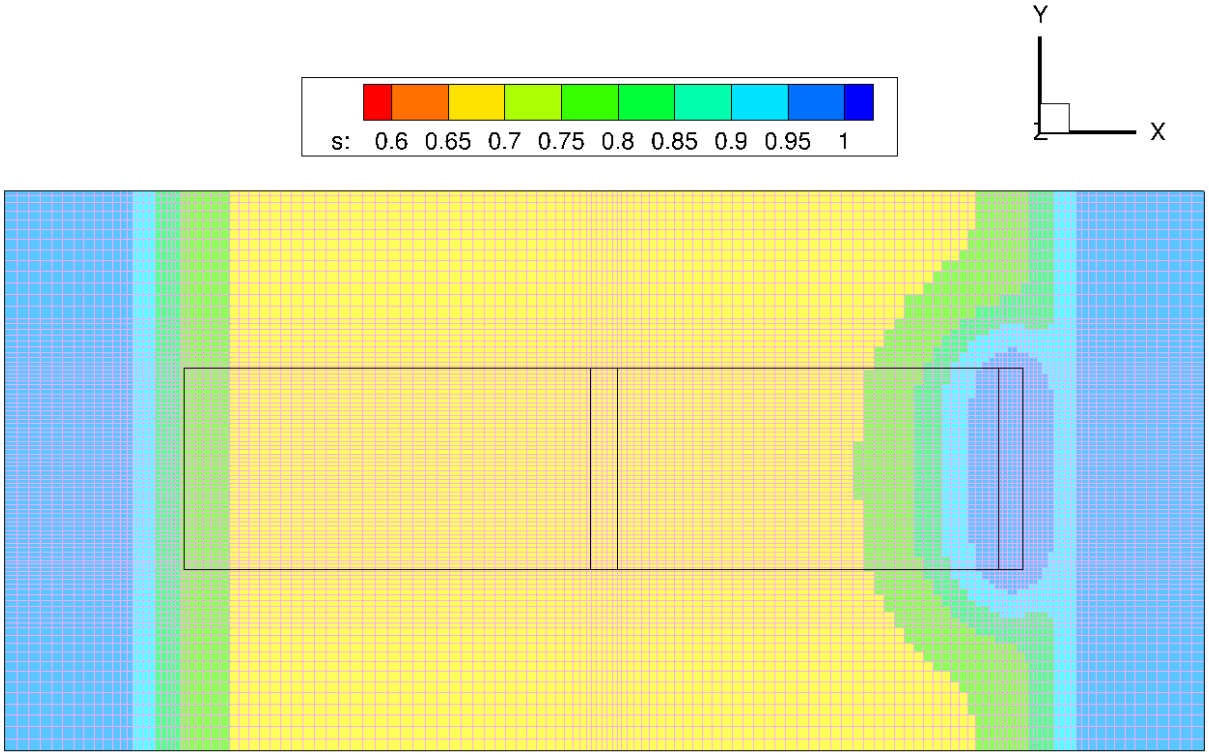

Figure 12. "End" saturation profile in the surface XY plane (i.e., a "birds-eye-view" of the disposal unit) with the disposal unit footprint and subsidence regions outlined in black.

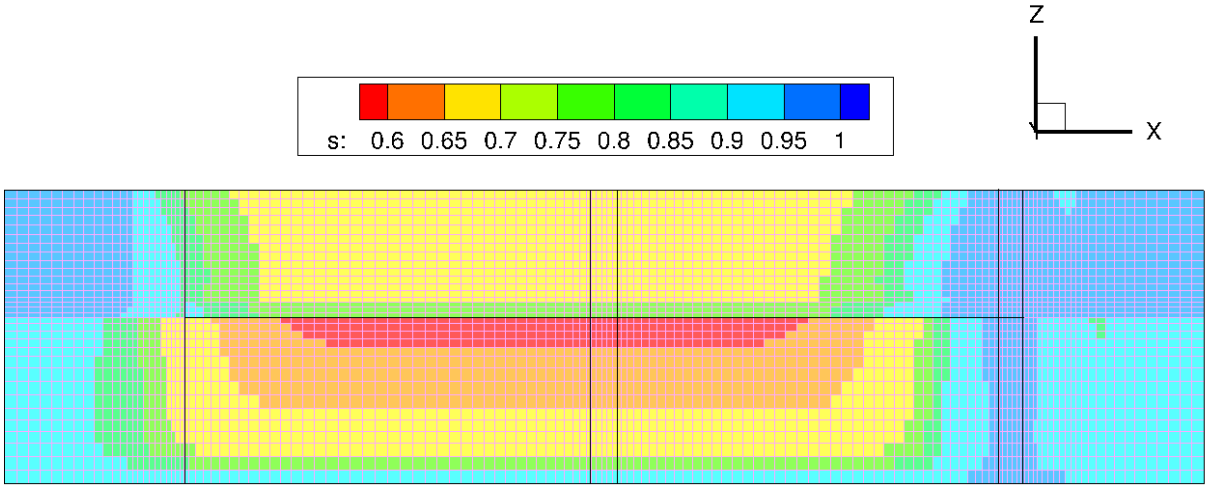

Figure 13. "End" saturation profile in the middle XZ plane (i.e., a cross-section extending from the ground surface to the water table) with the disposal unit footprint and subsidence regions outlined in black.

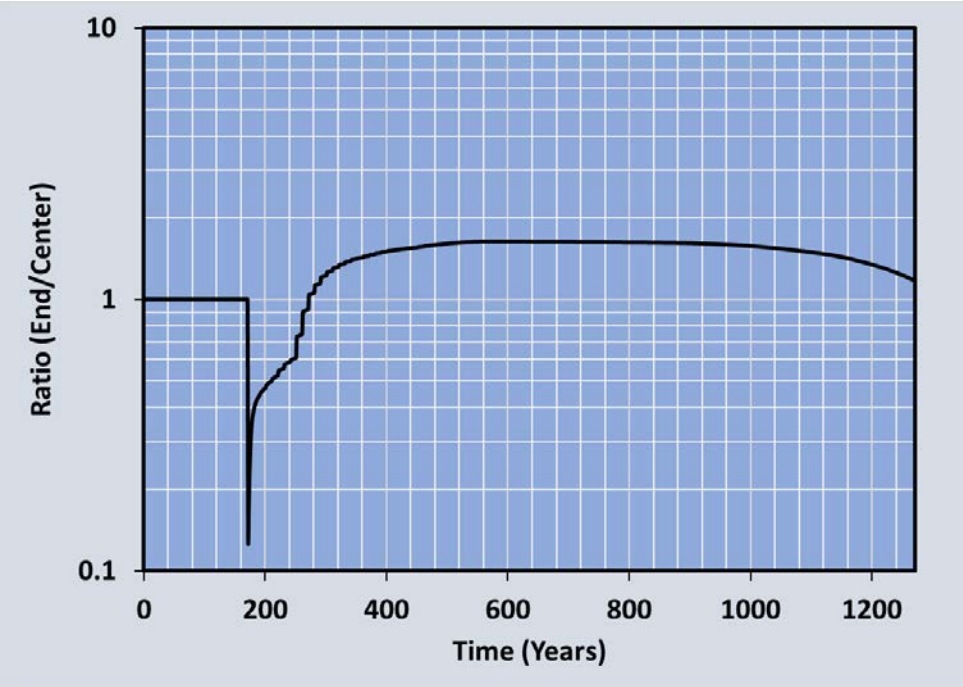

Figure 14. Ratio of the flux to the water table at each point in time (i.e., End:Center) for H-3.

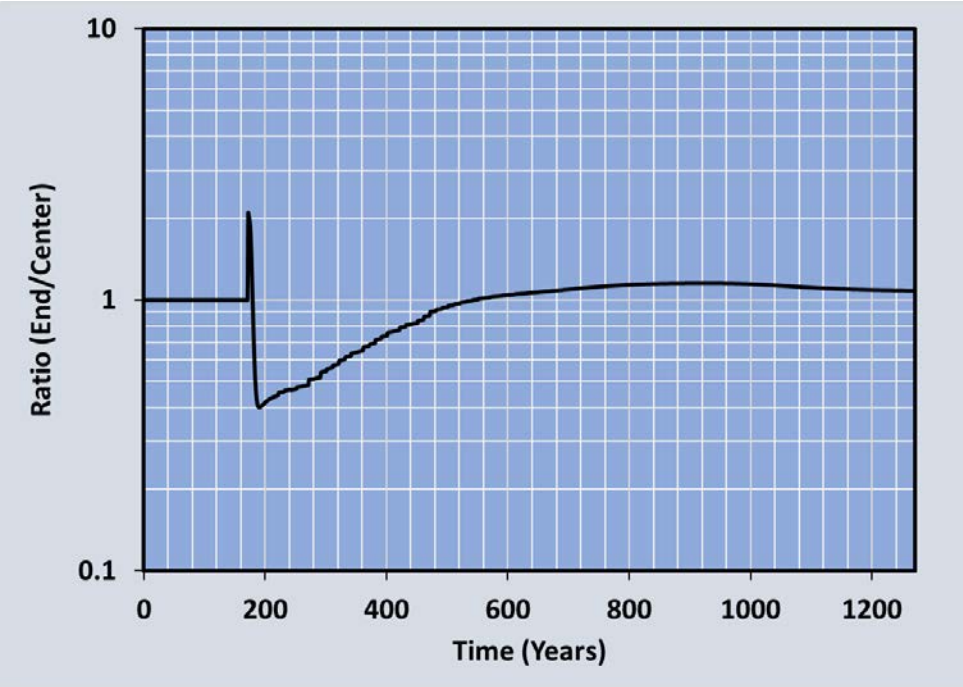

Figure 15. Ratio of the flux to the water table at each point in time (i.e., End:Center) for I-129.

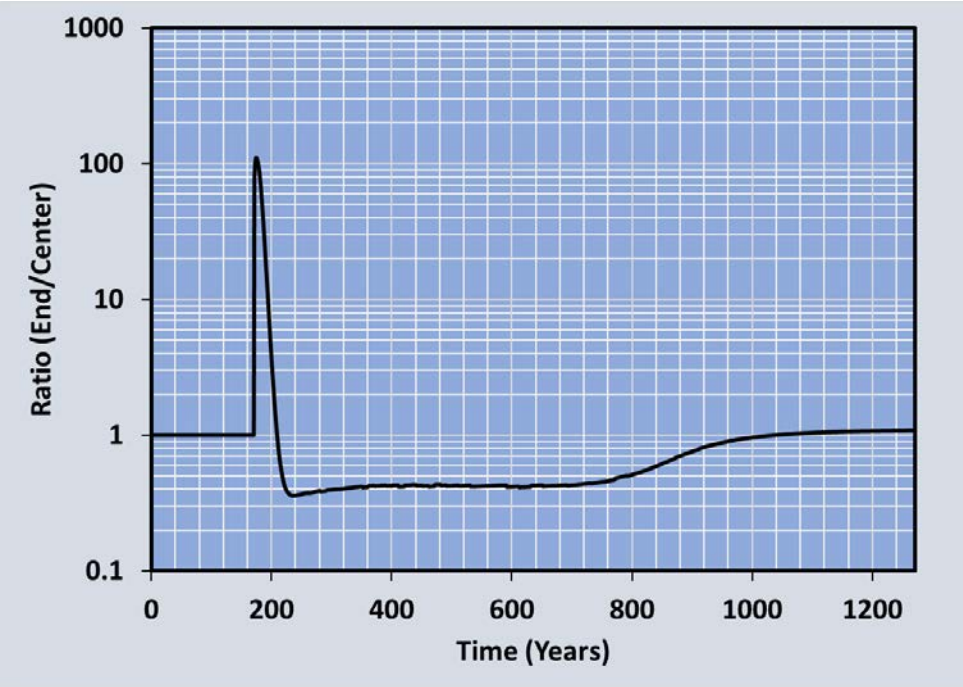

Figure 16. Ratio of the flux to the water table at each point in time (i.e., End:Center) for Sr-90.

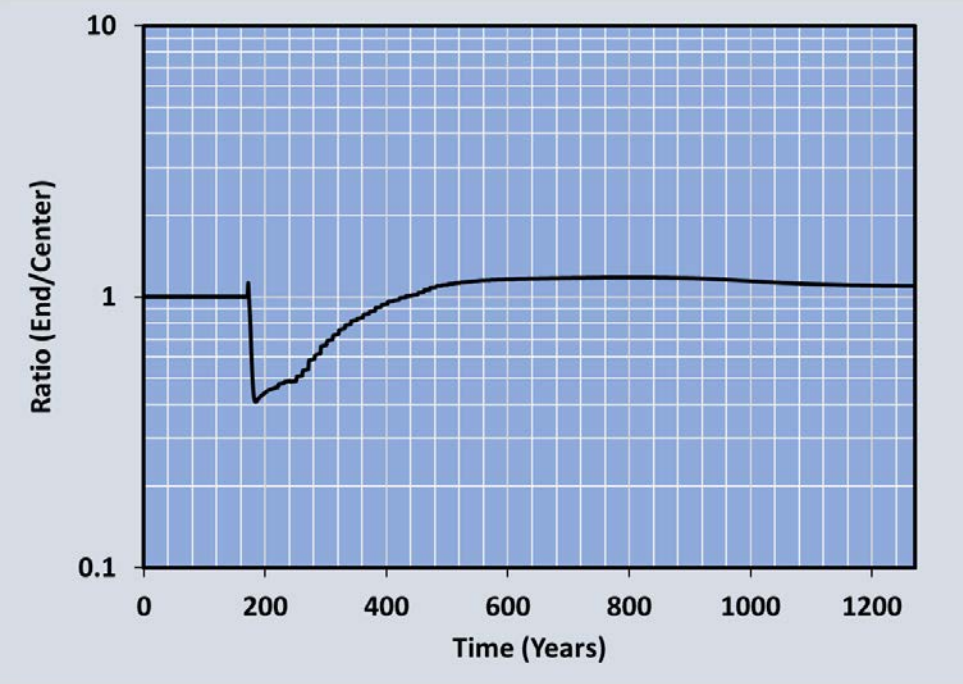

Figure 17. Ratio of the flux to the water table at each point in time (i.e., End:Center) for Tc-99.

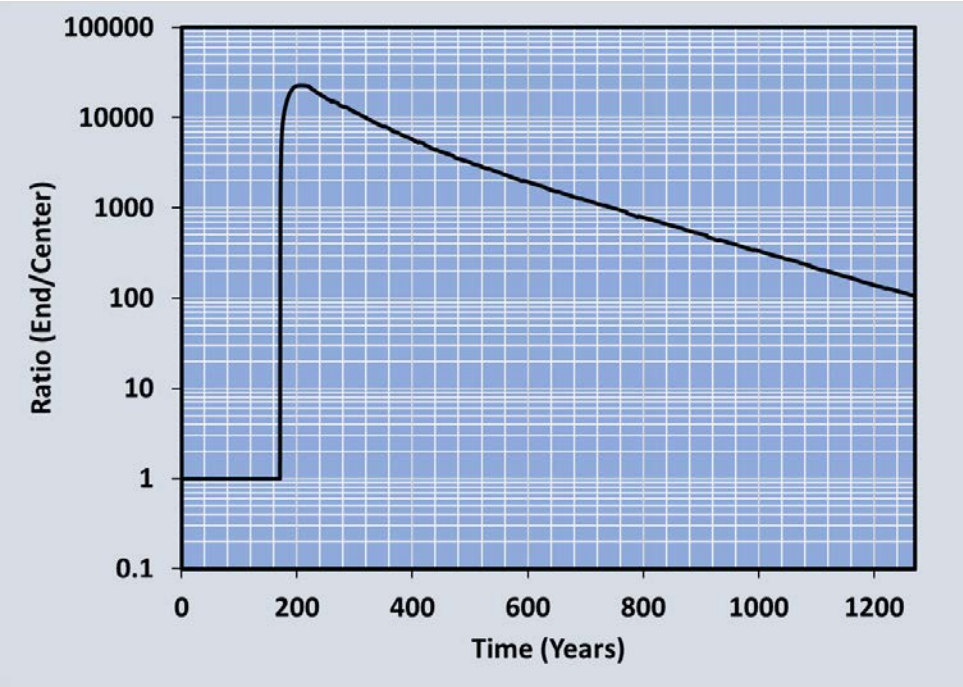

Figure 18. Ratio of the flux to the water table at each point in time (i.e., End:Center) for U-235.

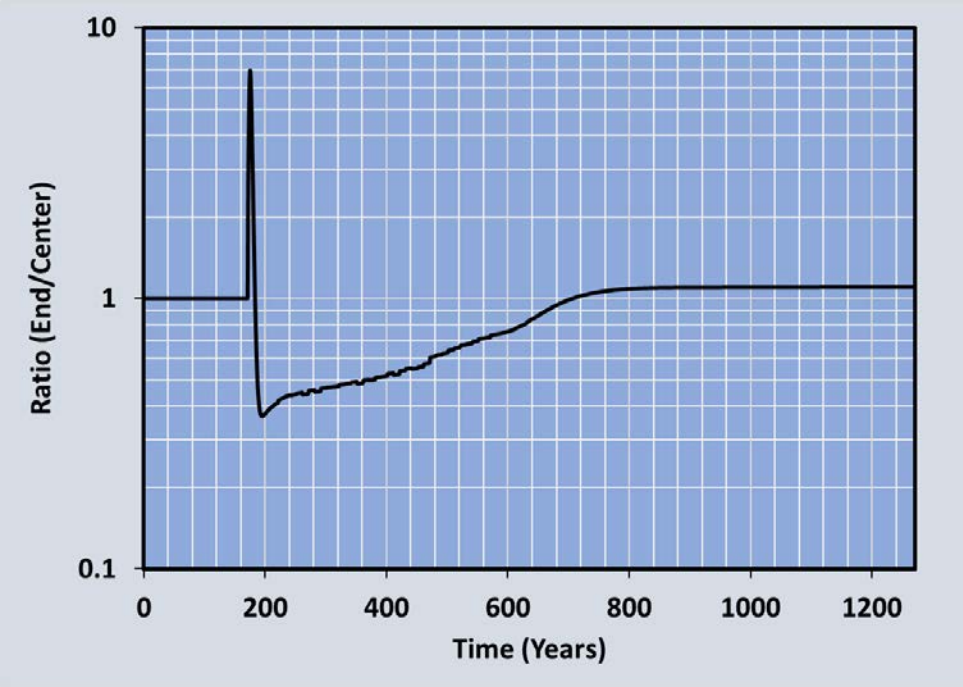

Figure 19. Ratio of the flux to the water table at each point in time (i.e., End:Center) for C-14.

References

ACRi 2018. PORFLOW User's Manual, *Keyword Commands Version 6.42.9, Revision 0*. Analytical & Computational Research, Inc., Los Angeles, CA, April 23, 2018.

Danielson, T. L. (2019) A Monte Carlo Rectangle Packing Algorithm for Identifying Likely Spatial Distributions of Final Closure Cap Subsidence in the E-Area Low Level Waste Facility. SRNL-STI-2019-00440, Rev. 0. Savannah River National Laboratory, Aiken, SC.

Dyer, J. A. (2018) Conceptual Modeling Framework for E-Area PA HELP Infiltration Model Simulations. SRNL-STI-2017-00678, Rev. 0. Savannah River National Laboratory, Aiken, SC.

Dyer, J. A., and Flach, G. P. (2018) Infiltration Time Profiles for E-Area LLWF Intact and Subsidence Scenarios. SRNL-STI-2018-00327, Rev. 0. Savannah River National Laboratory, Aiken, SC.

Nichols, R. L. (2019) Hydraulic Properties Data Package for the E-Area Soils, Cementitious Materials, and Waste Zones Update. SRNL-STI-2019-00355. Savannah River National Laboratory, Aiken, SC.

Appendix A

Table 3. Disposal dates for each package in the non-crushable package inventory and the corresponding fractional package placement time during the trench operations. Packages shown in red were reported to have been placed prior to the opening of the trench segment and were therefore considered to be placed at time 0.

Package ID	*Location*	*Unit*	*Disposal Date*	*Segment Open*	*Segment Close*	*Operating Delta t (days)*	*Package Placement Fractional Time*
CBALX4962	ETRENCH2	1	12/15/2010	6/3/2004	NA	5579	0.43
CBALX5066	ETRENCH2	1	2/24/2011	6/3/2004	NA	5579	0.44
CBALX5083	ETRENCH2	1	3/31/2011	6/3/2004	NA	5579	0.45
AC10001497	SLIT14	A	2/19/2011	4/14/2011	4/14/2011	1	0.00
RD009462	SLIT2	1	12/11/2002	9/20/2001	10/22/2003	762	0.59
RD009463	SLIT2	1	12/11/2002	9/20/2001	10/22/2003	762	0.59
RD009464	SLIT2	1	12/9/2002	9/20/2001	10/22/2003	762	0.58
RD009465	SLIT2	1	12/9/2002	9/20/2001	10/22/2003	762	0.58
RD009466	SLIT2	1	12/12/2002	9/20/2001	10/22/2003	762	0.59
RD009467	SLIT2	1	12/12/2002	9/20/2001	10/22/2003	762	0.59
RD009468	SLIT2	1	12/12/2002	9/20/2001	10/22/2003	762	0.59
RD009469	SLIT2	1	12/11/2002	9/20/2001	10/22/2003	762	0.59
WP24730001	SLIT2	A	9/24/2003	9/24/2003	8/31/2006	1072	0.00
SR595025	SLIT3	A	12/8/2003	10/20/2003	1/6/2004	78	0.64
SR595026	SLIT3	A	12/8/2003	10/20/2003	1/6/2004	78	0.64
WP24740033	SLIT3	B	1/6/2004	12/10/2003	4/21/2004	133	0.21
SR571645	SLIT3	C	2/23/2004	2/5/2004	4/15/2004	70	0.26
SR571683	SLIT3	C	2/23/2004	2/5/2004	4/15/2004	70	0.26
SR571687	SLIT3	C	2/23/2004	2/5/2004	4/15/2004	70	0.26
SR571688	SLIT3	C	2/23/2004	2/5/2004	4/15/2004	70	0.26
SR571691	SLIT3	C	2/23/2004	2/5/2004	4/15/2004	70	0.26
SR595027	SLIT3	C	2/23/2004	2/5/2004	4/15/2004	70	0.26
SR595032	SLIT3	C	2/23/2004	2/5/2004	4/15/2004	70	0.26
SR595033	SLIT3	C	2/23/2004	2/5/2004	4/15/2004	70	0.26
SR595035	SLIT3	C	2/23/2004	2/5/2004	4/15/2004	70	0.26
WP24740074	SLIT3	D	6/21/2004	3/23/2004	6/19/2007	1183	0.08
FD00009092	SLIT3	E	9/10/2004	7/20/2004	5/9/2005	293	0.18

Package ID	*Location*	*Unit*	*Disposal Date*	*Segment Open*	*Segment Close*	*Operating Delta t (days)*	*Package Placement Fractional Time*
FD00009093	SLIT3	E	8/31/2004	7/20/2004	5/9/2005	293	0.14
FD00009094	SLIT3	E	9/1/2004	7/20/2004	5/9/2005	293	0.15
FD00009095	SLIT3	E	9/1/2004	7/20/2004	5/9/2005	293	0.15
WP24740095	SLIT3	E	7/21/2004	7/20/2004	5/9/2005	293	0.01
WP24740192	SLIT3	E	12/6/2004	7/20/2004	5/9/2005	293	0.48
WP24740193	SLIT3	E	12/6/2004	7/20/2004	5/9/2005	293	0.48
WP24740194	SLIT3	E	12/4/2004	7/20/2004	5/9/2005	293	0.47
WP24740195	SLIT3	E	12/3/2004	7/20/2004	5/9/2005	293	0.47
WP24740196	SLIT3	E	12/3/2004	7/20/2004	5/9/2005	293	0.47
WP24740283	SLIT3	E	4/19/2005	7/20/2004	5/9/2005	293	0.93
ET11000640	SLIT3	F	2/10/2004	2/10/2004	2/10/2004	1	0.00
ET11000966	SLIT3	F	2/10/2004	2/10/2004	2/10/2004	1	0.00
ET11001003	SLIT3	F	2/10/2004	2/10/2004	2/10/2004	1	0.00
ET11001115	SLIT3	F	2/10/2004	2/10/2004	2/10/2004	1	0.00
FC30S01844	SLIT4	B	1/30/2007	1/10/2007	5/23/2007	133	0.15
SD00005112	SLIT4	B	2/14/2007	1/10/2007	5/23/2007	133	0.27
SD00005113	SLIT4	B	1/31/2007	1/10/2007	5/23/2007	133	0.16
SD00005114	SLIT4	B	1/31/2007	1/10/2007	5/23/2007	133	0.16
SD00005118	SLIT4	B	1/29/2007	1/10/2007	5/23/2007	133	0.15
SD00005119	SLIT4	B	1/25/2007	1/10/2007	5/23/2007	133	0.12
SD00005120	SLIT4	B	1/25/2007	1/10/2007	5/23/2007	133	0.12
SD00005121	SLIT4	B	1/24/2007	1/10/2007	5/23/2007	133	0.11
SD00005124	SLIT4	B	2/6/2007	1/10/2007	5/23/2007	133	0.21
SD00005132	SLIT4	B	2/6/2007	1/10/2007	5/23/2007	133	0.21
SD00006358	SLIT4	B	3/7/2007	1/10/2007	5/23/2007	133	0.42
SD00006383	SLIT4	B	3/22/2007	1/10/2007	5/23/2007	133	0.54
SD00006384	SLIT4	B	3/20/2007	1/10/2007	5/23/2007	133	0.52
SD00006386	SLIT4	B	3/22/2007	1/10/2007	5/23/2007	133	0.54
WP24740185	SLIT4	C	12/10/2004	12/10/2004	6/22/2005	194	0.00
WP24740186	SLIT4	C	12/10/2004	12/10/2004	6/22/2005	194	0.00
WP24740187	SLIT4	C	12/10/2004	12/10/2004	6/22/2005	194	0.00
WP24740188	SLIT4	C	12/10/2004	12/10/2004	6/22/2005	194	0.00

Package ID	*Location*	*Unit*	*Disposal Date*	*Segment Open*	*Segment Close*	*Operating Delta t (days)*	*Package Placement Fractional Time*
WP24740189	SLIT4	C	12/11/2004	12/10/2004	6/22/2005	194	0.01
WP24740190	SLIT4	C	12/11/2004	12/10/2004	6/22/2005	194	0.01
WP24740191	SLIT4	C	12/11/2004	12/10/2004	6/22/2005	194	0.01
WP24740209	SLIT4	C	5/23/2005	12/10/2004	6/22/2005	194	0.85
WP24740281	SLIT4	C	5/26/2005	12/10/2004	6/22/2005	194	0.86
WP24740282	SLIT4	C	5/26/2005	12/10/2004	6/22/2005	194	0.86
FD00009089	SLIT4	D	9/10/2004	8/3/2004	1/25/2005	175	0.22
FD00009096	SLIT4	D	9/10/2004	8/3/2004	1/25/2005	175	0.22
FD00009101	SLIT4	D	9/10/2004	8/3/2004	1/25/2005	175	0.22
SR571676	SLIT4	E	3/8/2004	2/26/2004	6/28/2004	123	0.09
SR571679	SLIT4	E	3/9/2004	2/26/2004	6/28/2004	123	0.10
SR571681	SLIT4	E	3/9/2004	2/26/2004	6/28/2004	123	0.10
SR571682	SLIT4	E	3/8/2004	2/26/2004	6/28/2004	123	0.09
SR571685	SLIT4	E	3/9/2004	2/26/2004	6/28/2004	123	0.10
SR571689	SLIT4	E	3/8/2004	2/26/2004	6/28/2004	123	0.09
SWD041258	SLIT5	A	10/13/2004	10/13/2004	4/7/2005	176	0.00
SWD041259	SLIT5	A	10/13/2004	10/13/2004	4/7/2005	176	0.00
SWD041260	SLIT5	A	10/13/2004	10/13/2004	4/7/2005	176	0.00
SWD041261	SLIT5	A	10/13/2004	10/13/2004	4/7/2005	176	0.00
SWD041262	SLIT5	A	10/13/2004	10/13/2004	4/7/2005	176	0.00
SWD041263	SLIT5	A	10/13/2004	10/13/2004	4/7/2005	176	0.00
WP24740107	SLIT5	A	10/13/2004	10/13/2004	4/7/2005	176	0.00
WP24740197	SLIT5	A	12/17/2004	10/13/2004	4/7/2005	176	0.37
WP24740198	SLIT5	A	12/17/2004	10/13/2004	4/7/2005	176	0.37
WP24740199	SLIT5	A	12/17/2004	10/13/2004	4/7/2005	176	0.37
WP24740200	SLIT5	A	12/17/2004	10/13/2004	4/7/2005	176	0.37
WP24740201	SLIT5	A	12/17/2004	10/13/2004	4/7/2005	176	0.37
CBALX4472	SLIT5	C	9/8/2005	8/22/2005	1/5/2006	136	0.13
SD00005424	SLIT5	E	3/23/2006	2/13/2006	8/31/2006	199	0.19
FC30S01803	SLIT5	H	5/2/2006	5/2/2006	10/16/2006	167	0.00
WP24740212	SLIT5	J	8/3/2005	7/18/2005	8/11/2005	24	0.69
WP24740214	SLIT5	J	8/3/2005	7/18/2005	8/11/2005	24	0.69

Package ID	*Location*	*Unit*	*Disposal Date*	*Segment Open*	*Segment Close*	*Operating Delta t (days)*	*Package Placement Fractional Time*
WP24740223	SLIT5	J	8/10/2005	7/18/2005	8/11/2005	24	0.97
SWD061506	SLIT6	A	9/12/2006	4/29/2006	3/18/2008	689	0.20
SWD061507	SLIT6	A	9/12/2006	4/29/2006	3/18/2008	689	0.20
SWD061508	SLIT6	A	9/12/2006	4/29/2006	3/18/2008	689	0.20
SWD061509	SLIT6	A	9/12/2006	4/29/2006	3/18/2008	689	0.20
SWD061510	SLIT6	A	9/12/2006	4/29/2006	3/18/2008	689	0.20
SWD061511	SLIT6	A	9/12/2006	4/29/2006	3/18/2008	689	0.20
SWD061512	SLIT6	A	9/12/2006	4/29/2006	3/18/2008	689	0.20
SWD061513	SLIT6	A	9/12/2006	4/29/2006	3/18/2008	689	0.20
SWD061514	SLIT6	A	9/12/2006	4/29/2006	3/18/2008	689	0.20
SWD061515	SLIT6	A	9/12/2006	4/29/2006	3/18/2008	689	0.20
SWD061516	SLIT6	A	9/12/2006	4/29/2006	3/18/2008	689	0.20
SWD061517	SLIT6	A	9/12/2006	4/29/2006	3/18/2008	689	0.20
SWD061518	SLIT6	A	9/12/2006	4/29/2006	3/18/2008	689	0.20
SWD061519	SLIT6	A	9/12/2006	4/29/2006	3/18/2008	689	0.20
SWD061520	SLIT6	A	9/12/2006	4/29/2006	3/18/2008	689	0.20
SWD061521	SLIT6	A	9/12/2006	4/29/2006	3/18/2008	689	0.20
SWD061522	SLIT6	A	9/12/2006	4/29/2006	3/18/2008	689	0.20
SWD061523	SLIT6	A	9/12/2006	4/29/2006	3/18/2008	689	0.20
SWD061524	SLIT6	A	9/12/2006	4/29/2006	3/18/2008	689	0.20
SWD061525	SLIT6	A	9/12/2006	4/29/2006	3/18/2008	689	0.20
SWD061526	SLIT6	A	9/13/2006	4/29/2006	3/18/2008	689	0.20
SWD061527	SLIT6	A	9/13/2006	4/29/2006	3/18/2008	689	0.20
SWD061528	SLIT6	A	9/13/2006	4/29/2006	3/18/2008	689	0.20
SWD061529	SLIT6	A	9/13/2006	4/29/2006	3/18/2008	689	0.20
SWD061530	SLIT6	A	9/13/2006	4/29/2006	3/18/2008	689	0.20
SWD061531	SLIT6	A	9/13/2006	4/29/2006	3/18/2008	689	0.20
SWD061532	SLIT6	A	9/13/2006	4/29/2006	3/18/2008	689	0.20
SWD061533	SLIT6	A	9/13/2006	4/29/2006	3/18/2008	689	0.20
SWD061535	SLIT6	A	9/13/2006	4/29/2006	3/18/2008	689	0.20
SWD061537	SLIT6	A	9/13/2006	4/29/2006	3/18/2008	689	0.20
SWD061538	SLIT6	A	9/13/2006	4/29/2006	3/18/2008	689	0.20

Package ID	*Location*	*Unit*	*Disposal Date*	*Segment Open*	*Segment Close*	*Operating Delta t (days)*	*Package Placement Fractional Time*
SWD061539	SLIT6	A	9/13/2006	4/29/2006	3/18/2008	689	0.20
SWD061540	SLIT6	A	9/13/2006	4/29/2006	3/18/2008	689	0.20
SWD061541	SLIT6	A	9/13/2006	4/29/2006	3/18/2008	689	0.20
SWD061542	SLIT6	A	9/13/2006	4/29/2006	3/18/2008	689	0.20
SD00005127	SLIT6	B	11/6/2006	11/1/2006	2/1/2007	92	0.06
SD00005129	SLIT6	B	11/27/2006	11/1/2006	2/1/2007	92	0.29
SD00005131	SLIT6	B	11/27/2006	11/1/2006	2/1/2007	92	0.29
CBALX4760	SLIT6	C	7/29/2008	5/27/2008	6/23/2010	757	0.08
CBALX4776	SLIT6	C	7/9/2008	5/27/2008	6/23/2010	757	0.06
CBALX4783	SLIT6	C	7/24/2008	5/27/2008	6/23/2010	757	0.08
CBALX4845	SLIT6	C	11/12/2008	5/27/2008	6/23/2010	757	0.22
FCAN08001	SLIT6	C	7/23/2008	5/27/2008	6/23/2010	757	0.08
AC10001498	SLIT6	D	2/9/2011	2/1/2011	3/12/2011	39	0.22
AC10001499	SLIT6	D	2/11/2011	2/1/2011	3/12/2011	39	0.27
FC30S01824	SLIT6	F	10/30/2006	10/30/2006	6/15/2010	1324	0.00
SD00005128	SLIT6	F	12/7/2006	10/30/2006	6/15/2010	1324	0.03
SD00005130	SLIT6	F	12/7/2006	10/30/2006	6/15/2010	1324	0.03
FCASROX100	SLIT6	G	7/21/2010	7/21/2010	12/2/2010	134	0.00
RD00009839	SLIT7	E	8/1/2006	6/26/2006	12/13/2006	170	0.21
SWD061534	SLIT7	E	10/17/2006	6/26/2006	12/13/2006	170	0.67
SWD061536	SLIT7	E	10/17/2006	6/26/2006	12/13/2006	170	0.67
SWD061500	SLIT7	F	3/5/2007	6/28/2006	6/11/2007	348	0.72
SWD061501	SLIT7	F	3/5/2007	6/28/2006	6/11/2007	348	0.72
SWD061502	SLIT7	F	3/5/2007	6/28/2006	6/11/2007	348	0.72
SWD061503	SLIT7	F	3/5/2007	6/28/2006	6/11/2007	348	0.72
SWD061504	SLIT7	F	3/5/2007	6/28/2006	6/11/2007	348	0.72
SWD061505	SLIT7	F	3/5/2007	6/28/2006	6/11/2007	348	0.72
HC27001821	SLIT7	H	6/17/2008	9/26/2007	9/30/2008	370	0.72
ET11001154	SLIT7	J	2/3/2009	2/3/2009	9/1/2010	575	0.00
SD00006680	SLIT7	K	3/8/2010	3/8/2010	7/28/2010	142	0.00
SD00006313	SLIT8	B	2/12/2007	2/13/2007	3/14/2007	29	0.00

Distribution List

S. E. Aleman, 735-A
B. T. Butcher, 773-42A
D. A. Crowley, 773-42A
T. L. Danielson, 773-42A
K. L. Dixon, 773-42A
J. A. Dyer, 773-42A
L. L. Hamm, 735-A
T. Hang, 773-42A
C. C. Herman, 773-A
J. J. Mayer, 999-W
R. L. Nichols, 773-42A
A. P. Fellinger, 773-42A
T. S. Whiteside, 773-42A
J. L. Wohlwend, 773-42A
T. N. Foster, EM File, 773-42A – Rm. 243
Records Management (EDWS)